Surface roughness and removal rate in magnetorheological finishing of a subsurface damage free surface*

CHENG Haobo[1 **], WANG Yingwei[2], FENG Zhijing[1] and CHENG Kai[3]

(1. State Key Laboratory of Tribiology, Tsinghua University, Beijing 100084, China; 2. Department of Material Sciences, Changchun University of Science and Technology, Changchun 130021, China; 3. Faculty of Information and Engineering Systems, City Campus, Leeds LS1 3HE, UK)

Received October 9, 2004; revised November 2, 2004

Abstract Based on computer-controlled optical surfacing, a new technique called magnetorheological finishing (MRF), is presented. The new technique combines the features of conventional loose abrasive machining with a wheel shaped polishing tool. The tool incorporates a host of features and has unprecedented fabricating versatility. The pre-polishing and fine polishing processes can be performed only by adjusting different parameters. The material removal function is studied theoretically and the results of simulation present a Gaussian distribution feature. Based on the established theoretical model, material removal rate experiments involving a parabolic mirror are designed and carried out to determine the effect of controllable parameters on size of the gap between the workpiece and the polishing wheel, rotating speed of the polishing wheel, concentration of volume fraction of non-magnetic particles and polishing time. Further experiments are carried out on the surface microstructure of the workpiece, the final surface roughness with an initial value of 10.98 nm reaches 1.22 nm root mean square (RMS) after 20 min of polishing. The subsurface damage experiment and the atomic force microscopy (AFM) measurement on the polished surface can also verify the feasibility of the MRF technique.

Keywords: magnetorheological finishing, surface roughness, computer controlled optical surfacing, subsurface damage, removal function.

Aspherical optical components are important in modern optical systems[1]. There exist many types of aspheres. The commonly used ones include parabola, ellipsoid, etc.[2] Recently, increasing requirements for aspherical optical components (e.g. for lithography) together with growing fields of their application (e.g. conformal and freeform optics) result in a strong need for optical finishing methods that can be applied locally to polish complex shaped aspheres in brittle materials (e.g. glass)[3]. However, making high-precision aspheres is still primarily an arduous, labor-intensive process. In the traditional finishing process, components close to the desired size is firstly made by a cutting machine but with a very low-precision, and then an expert optician performs most of the work manually. The optician usually uses a precisely shaped lap, a conventional rigid lap, which is made of pitch or polyurethane[4]. This transfers pressure through an abrasive slurry to the entire surface material of the components. Material is then removed by chemical and mechanical interactions between the abrasive and the components. However, the removal rate is slow and so the time to fabricate high-precision optical components is long[5]. Currently aspherical optical surfaces are usually finished by computer-controlled polishing with subaperture pads[6—8]. Computer-controlled polishing applies the traditional finishing process of loose abrasive load controlled polishing[9]. This is a three-body process in which abrasive particles (suspended in a fluid) are pressed against the optical surface by a deformable polishing tool, and material is removed by a chemomechanical process[10]. Alternatively, minimizing the contact area between the tool and the surface, elastic emission machining (EEM)[11] is a float polishing process[12] in which the tool is floating on the liquid layer containing the abrasive particles. The thickness of this liquid layer amounts to a multiple of the diameter of the abrasive particles[13], and the determining parameters of the process include the hydraulic pressure generated by the tool and the kinetic energy of the abrasives. With surface roughness requirements of better than 1 nm RMS commonly in supersmooth optics, component specifications often exceed the capabilities of commercial high speed optical fabrication equipment[14].

* Supported by National Natural Science Foundation of China (Grant No. 50175062) and the National High Technology Research and Development Program of China (Grant No. 2001AA421140)

** To whom correspondence should be addressed. E-mail: chenghb@tsinghua.edu.cn

In this paper, we report a novel subaperture polishing and shaping technique, called magnetorheological finishing (MRF). A MRF system is developed to overcome the limitation of the current MRF technique which is mostly applied to polish medium or small size optical elements[15]. The distinguished characteristic of the designed MRF system lies in a small polishing wheel with horizontal axis. The wheel rotates around the axis and the axis rotates around the center of the wheel in a horizontal plane. The wheel is mounted downwards scanning the workpiece as a subaperture tool, especially fit for polishing asymmetric parts, i.e. conformal and freeform lens. A part is installed on a turntable upwards which is helpful to reduce the rotational inertia when polishing large size workpieces. For the novel MRF system, the mathematics model of finishing optics is established on the basis of Preston equation[16], then simulation on the features of material removal function is also carried out. Finally, experiments are performed to analyze the process of polishing of optical components by MRF.

1 MRF technology

In MRF, magnetically stiffened magnetorheological (MR) fluid flows through a preset converging gap which is formed by a workpiece surface and a moving rigid wall, to create precise material removal and polishing. A fundamental advantage of MRF over traditional polishing is that the polishing tool does not wear, since the re-circulated fluid is continuously monitored and maintained. Therefore, during polishing, the material removal function is not changed, that is useful for control of the polishing process. From the above description, it can be understood that there are two preconditions for successful MRF: one is presenting a suitable gradient magnetic field, the other is preparing MR fluid with good rheology.

1.1 Tool for MRF and its structure

Fig. 1(a) and (b) show the structure of the wheel shaped polishing tool and the distribution of magnets on the tool, which are mounted on the MRF system developed in-house. During the fabricating process, the wheel shaped polishing tool is driven by one motor through a belt along its self-rotating axis, and at the same time, another motor drives the polishing wheel which has a co-rotating axis. Thus, the surface material of the workpiece can be removed by virtue of self-rotating motion. On the other hand, the co-rotating motion will also change the manufacturing orbit continually, which is also an innovative feature of the system. The magnets are distributed on both sides of the magnetproof plate symmetrically as shown in Fig. 1(b), in order to make the magnetic line cross the working gap between the polishing wheel and the workpiece, keep the gradient direction of magnetic field as perpendicular to the surface of the workpiece as possible.

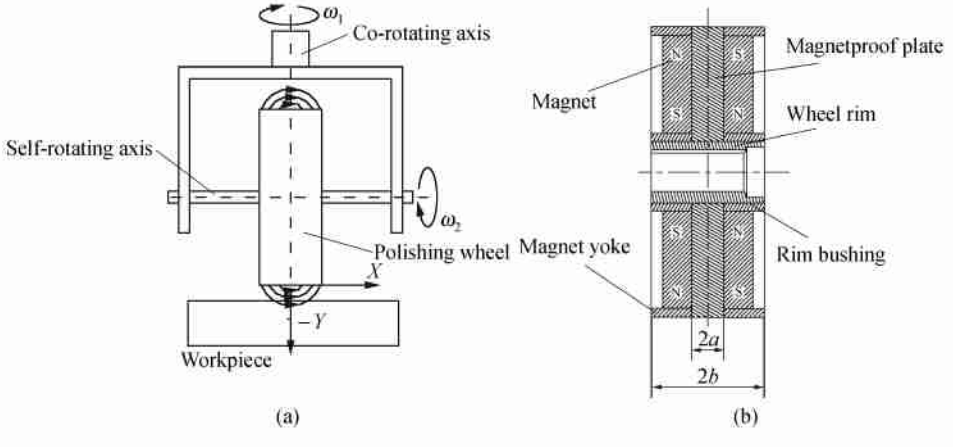

Fig. 1. Moving schematic (a) and magnet distribution (b) views of the polishing wheel.

1.2 Principle and model of MRF

During polishing, as shown in Fig. 2, a workpiece is immersed in MR fluid at a fixed distance from the polishing wheel. When the MR fluid is delivered into the working gap between the workpiece and the polishing wheel, it will stiffen under the action of the magnetic field gradient, and become a plastic Bingham medium. Thereafter, a shear flow of the plastic MR fluid produces a high pressure (or high stress) on a portion of the surface of the workpiece, which can result in the material removal. Since the polishing

tool is small in diameter, the area, where material removal occurs is designated as the 'polishing spot'.

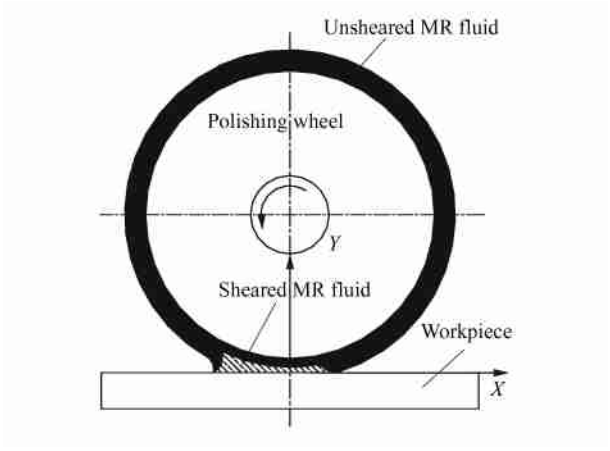

Fig. 2. Schematic diagram of the principle of MRF.

Based on the Preston equation, which is commonly accepted in optical manufacturing, a mathematic model of MRF is established. According to Preston, the rate of material removal is

$$\boldsymbol{L}(x,y)=k\boldsymbol{P}(x,y)\boldsymbol{V}(x,y), \tag{1}$$

where k is the Preston coefficient, $\boldsymbol{P}$ is the pressure on the surface of the workpiece in the polishing spot, $\boldsymbol{V}$ is the velocity of MR fluid in the polishing spot. In the model, $\boldsymbol{P}$ is a very complicated parameter and it is made up of the hydrodynamic pressure $\boldsymbol{P}_{\mathrm{f}}$ and magnetic pressure $\boldsymbol{P}_{\mathrm{m}}$. MR fluid is incompressible, and the magnetic deformation pressure can be ignored. So, magnetic pressure is mainly produced by magnetization. The expression of $\boldsymbol{P}$ is[17]

$$\boldsymbol{P}=\boldsymbol{P}_{\mathrm{m}}+\boldsymbol{P}_{\mathrm{f}}. \tag{2}$$

For the wheel shaped polishing tool presented in Fig. 1(a), the magnetic paths beside the magnetproof plate can be developed theoretically as shown in Fig. 1(b). Therefore, the distribution of magnetic intensity can be expressed as

$$\begin{cases}\boldsymbol{H}=\sum_{n=1}^{\infty}-A_n\cos(\beta_n x)\mathrm{e}^{-\beta_n y i}+\sum_{n=1}^{\infty}A_n\sin(\beta_n x)\mathrm{e}^{-\beta_n y j},\\ A_n=K_n\beta_n=\dfrac{2B_{\mathrm{g}}\sin(\beta_n a)}{\pi(2n-1)\mu_0},\\ \beta_n=\dfrac{2n-1}{2b}\pi,\\ K_n=\dfrac{4b\cdot B_{\mathrm{g}}\cdot\sin(\beta_n a)}{\pi^2\cdot(2n-1)^2\cdot\mu_0},\quad n=1,2,3,\cdots,\end{cases} \tag{3}$$

where $\boldsymbol{H}$ is the magnetic intensity, n is the iterative order number, A_n, β_n, K_n are coefficients, a is half width of the magnetproof plate, b is half width of the polishing wheel, B_{g} is magnetic induction intensity, and μ_0 is the vacuum permeability. In the magnetic field, magnetic particles will aggregate. Considering the interaction force, a spherical carbonyl iron particle of radius r and magnetic permeability μ_{p} has a magnetic moment of[18]

$$m=4\pi\mu_0\mu_{\mathrm{f}}r^3\frac{\mu_{\mathrm{p}}-\mu_{\mathrm{f}}}{\mu_{\mathrm{p}}+2\mu_{\mathrm{f}}}H, \tag{4}$$

where μ_{f} is the magnetic permeability of the host liquid. For the volume fraction ϕ of the magnetic particles in MR fluid, the magnetization of the host liquid is approximately[19]

$$M_{\mathrm{f}}=\phi M=m/V=3m/(4\pi r^3). \tag{5}$$

The magnetic pressure $\boldsymbol{P}_{\mathrm{m}}$ can be expressed as

$$\begin{aligned}\boldsymbol{P}_{\mathrm{m}}&=\mu_0\int_0^H M_{\mathrm{f}}(H)\mathrm{d}H\\&=3\phi\mu_0\mu_{\mathrm{f}}\frac{\mu_{\mathrm{p}}-\mu_{\mathrm{f}}}{\mu_{\mathrm{p}}+2\mu_{\mathrm{f}}}\int_0^H H\mathrm{d}H.\end{aligned} \tag{6}$$

Given the least distance between the polishing wheel and the workpiece h_{m}, R is the radius of the polishing wheel. According to the theory of hydrodynamic lubrication, hydrodynamic pressure $\boldsymbol{P}_{\mathrm{f}}$ can be simplified as[20]

$$\begin{aligned}\frac{\mathrm{d}\boldsymbol{P}_{\mathrm{f}}}{\mathrm{d}x}&=6\eta\boldsymbol{U}\frac{h-h^*}{h^3}\\&=6\eta\boldsymbol{U}\frac{2Rh_{\mathrm{m}}+x^2-2Rh^*}{2Rh^3},\end{aligned} \tag{7}$$

where h is the distance between the polishing wheel and a random point on the sample surface, $\boldsymbol{U}$ is the linear speed of the polishing tool, η is the original viscosity of MR fluid, and h^* is the distance between the points on sample surface, where the hydrodynamic pressure has its maximum value, and the shearing flow fluid. Let

$$\tan\gamma=x/\sqrt{2Rh_{\mathrm{m}}},\quad \boldsymbol{P}_{\mathrm{f}}=\frac{h_{\mathrm{m}}^2\boldsymbol{P}_{\mathrm{f}}}{6\eta\boldsymbol{U}\sqrt{2Rh_{\mathrm{m}}}},$$

where γ is the angle between the tangent line of sheared MR fluid and the surface of the workpiece, $\overline{\boldsymbol{P}_{\mathrm{f}}}$ is the distribution of pressure on the sample surface. Under the boundary condition of

$$\begin{cases}\gamma=-\pi/2,\quad(x=-\infty),\\ \gamma^*=25^\circ25',\quad \boldsymbol{P}_{\mathrm{f}}=0,\ \mathrm{d}\boldsymbol{P}_{\mathrm{f}}/\mathrm{d}x=0,\end{cases}$$

$$\boldsymbol{P}_{\mathrm{f}}=\frac{0.32275}{8}\left(\gamma+\frac{\pi}{2}\right)-\frac{0.22575\sin2\gamma}{4}-\frac{1.22575\sin4\gamma}{32}. \tag{8}$$

So, in two-dimensional coordinates, the distribution of pressure on the sample surface is obtained.

2 Material removal function simulation

Substituting Eq. (6) and Eq. (8) into Eq. (1), the rate of material removal can be drawn out

$$\boldsymbol{L} = k\left\{3\phi\mu_0\mu_f\frac{\mu_p-\mu_f}{\mu_p+2\mu_f}\int_0^H H\mathrm{d}H+\frac{0.32275}{8}\left(\gamma+\frac{\pi}{2}\right)-\frac{0.22575\sin 2\gamma}{4}-\frac{1.22575\sin 4\gamma}{32}\right\}\boldsymbol{V}. \tag{9}$$

Based on the basic Preston statement, in the polishing process, the material removal function with a central peak smoothly decreases to zero, which will make the workpiece surface quickly converge to the desired high quality optical surface[21]. The material removal function should have a Gaussian distribution function in computer controlled optical surfacing (CCOS). The characteristic of the obtained material removal function from Eq. (9) has been investigated (Fig. 3).

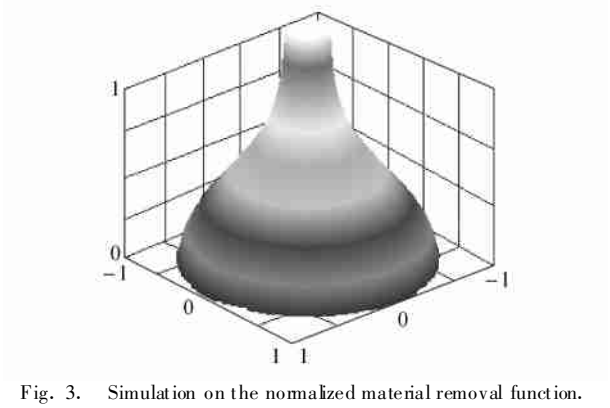

Fig. 3. Simulation on the normalized material removal function.

3 Experimental details

3.1 Features of material removal rate

Research on the effect of MRF is carried out. The parameters include the size of the gap between the workpiece and the polishing wheel, the rotating speed of the polishing wheel, and the concentration of the volume fraction of the non-magnetic particles and polishing time. In the process, a K9 parabolic mirror ($K = 4.8\times 10^{-13}$ m^2/N) is chosen as a test-part. Detailed working conditions are as follows: the magnetic density is $B_g = 0.32$ T, oil based MR fluid components in terms of ratio of volume to concentration are: 26.18% carbonyl iron particle (permeability $\mu_p = 1500$), 61% oil, and 2.82% stabilizing agent (silicon oil).

The values of experimental parameters used are shown in Table 1. From Fig. 4, the material removal rates, measured on a coordinate measuring machine (CMM) with a resolution of 0.1 μm, are found to be sensitive to four parameters: size of gap, speed of polishing wheel, volume fraction of cerium oxide (CeO_2) and polishing time. Especially for the size of gap, the material removal decreases with the increasing of the gap size and the material removal rate is virtually linearly proportional to the three other parameters (Fig. 4).

Table 1. Experimental conditions

Number	Size of gap (mm)	Rotational speed of the tool (rpm)	Volume of CeO_2(%)	Time (s/cycle)
1	0.8—2.0	180	6	120
2	1.0	0—260	6	120
3	1.0	180	2—10	120
4	1.0	180	6	0—150

3.2 Features of material removal function

To clearly understand the characteristics of material removal during the actual polishing process, it is necessary to carry out a fixed-point polishing experiment under a preset condition. Only in this way can a correct and practical-situation-meeting experimental result be achieved. According to this issue, the detailed experimental parameters are designed as: the radius of the polishing wheel is 33 mm, the gap size is 1 mm, the original viscosity of the polishing fluids is 0.5 Pa·s, the magnetic permeability of carbonyl iron particle is 1500, the rotating speed of the polishing wheel is 180 rpm, and the polishing time is 150 second.

The material removal distribution features measured by a Talysurf Plus (Fig. 5) present a sharp Gaussian distribution characteristic with a higher center peak. The smoothly outward expanding trend also reflects the stable removal feature of the MRF technique. The ability of MRF to remove mass from a surface is necessary to accomplish figure correction, but is not sufficient: MRF must also smooth away surface roughness quickly.

Figure 6 shows the evolution of surface roughness with elapsed finishing time measured with non-contacting optical profilometry. Two methods are conducted to illustrate the smoothing capability of the proposed MRF system. In the one method, self-rotation of the polishing wheel around its axis is used without co-rotation. Meanwhile, the sample held on

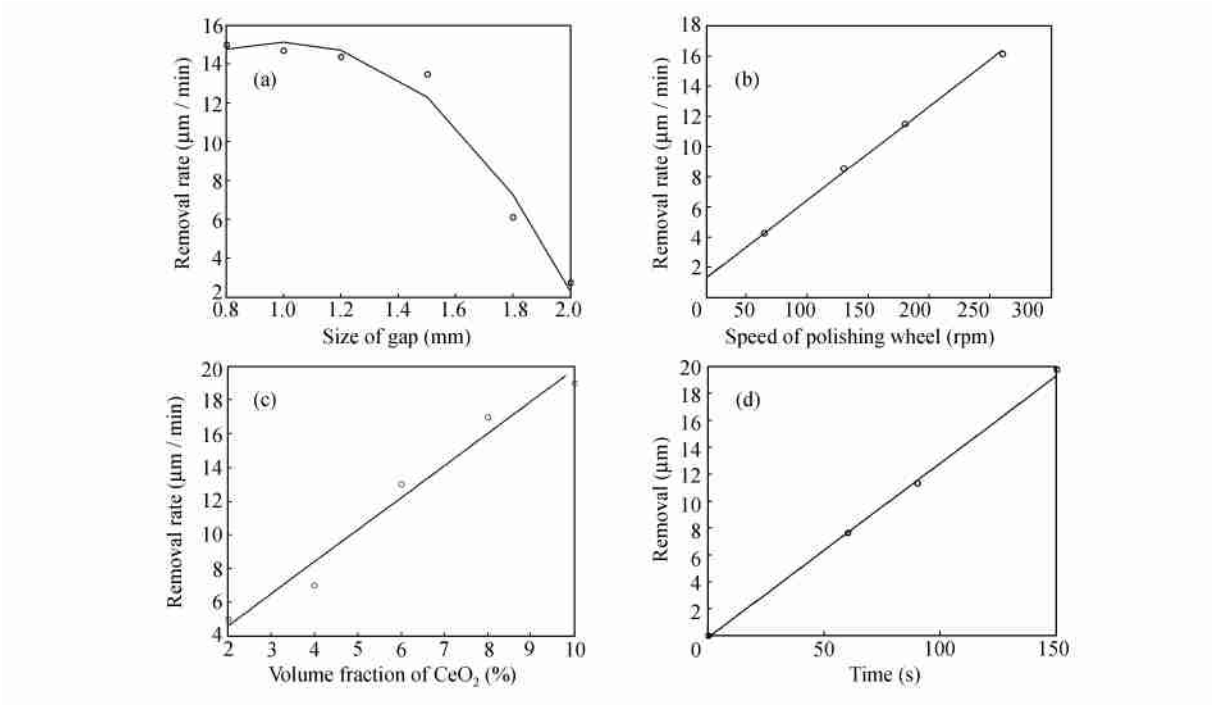

Fig. 4. Effects of several parameters on the material removal rate.

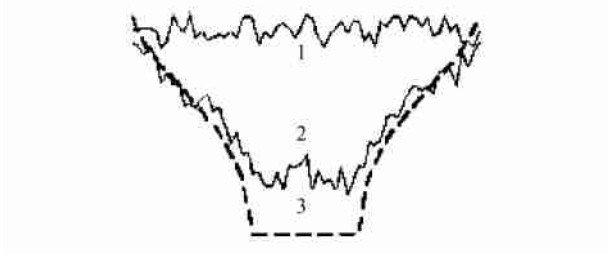

Fig. 5. Material removal function features of the fixing-point polishing area measured by Talysurf Plus. (1) Original figure; (2) figure after polishing; (3) desired figure.

a turntable is rotated at a constant speed. The smoothing results correspond to curve 1 in Fig. 6. In the other method, the self-rotation of the wheel shaped polishing tool is combined with its relatively low speed co-rotation, and the smoothing results correspond to curve 2 in Fig. 6. The smoothing process is sensitive to the size of CeO_2 abrasive. Using the above two methods, as shown in Fig. 6(a), the MR fluid containing 1.0μm CeO_2 does not work well in smoothing. The MR fluid is adjusted to improve the surface roughness by substituting 0.3μm CeO_2 for 1.0μm CeO_2. The final RMS surface roughness, independent of the above two methods, is around 1 nm RMS. However, the surface roughness convergent time of the second method decreases from 30 min to 20 min (Fig. 6(b)).

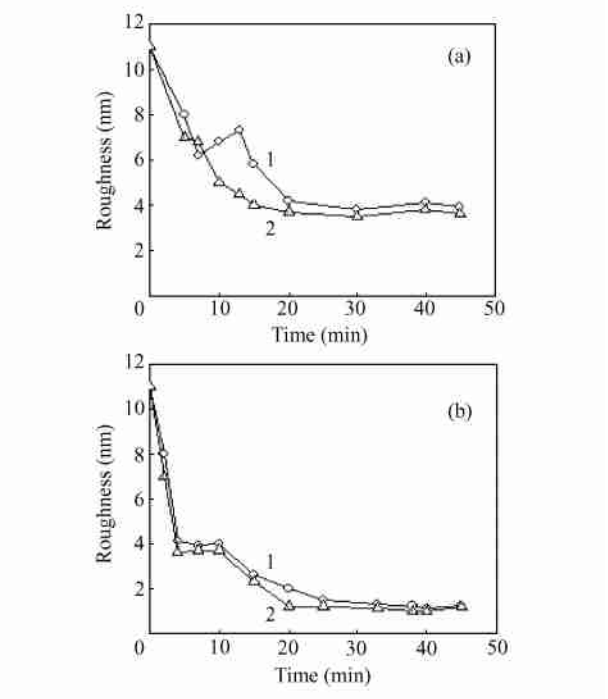

Fig. 6. Curves of surface roughness convergent with time. (a) 1μm abrasive; (b) 0.3μm abrasive.

For further analyzing the microstructure of the sample after MRF, the MR fluid containing 0.3μm CeO_2 is used for polishing. Comparison of Fig. 7(a) with Fig. 7(b) shows that there is a great improve-

ment on surface roughness of the sample after 10 min MRF (from Ra=10.98 nm to Ra=2.31 nm). This also verifies that MRF can rapidly remove material. However, there is obviously unsmooth transition between high points and low ones in Fig. 7(b). To remove this phenomenon, a second cycle polishing for 10 min is employed (Fig. 7(c)). The value of surface roughness decreases to Ra=1.22 nm, and the large high regions are largely removed.

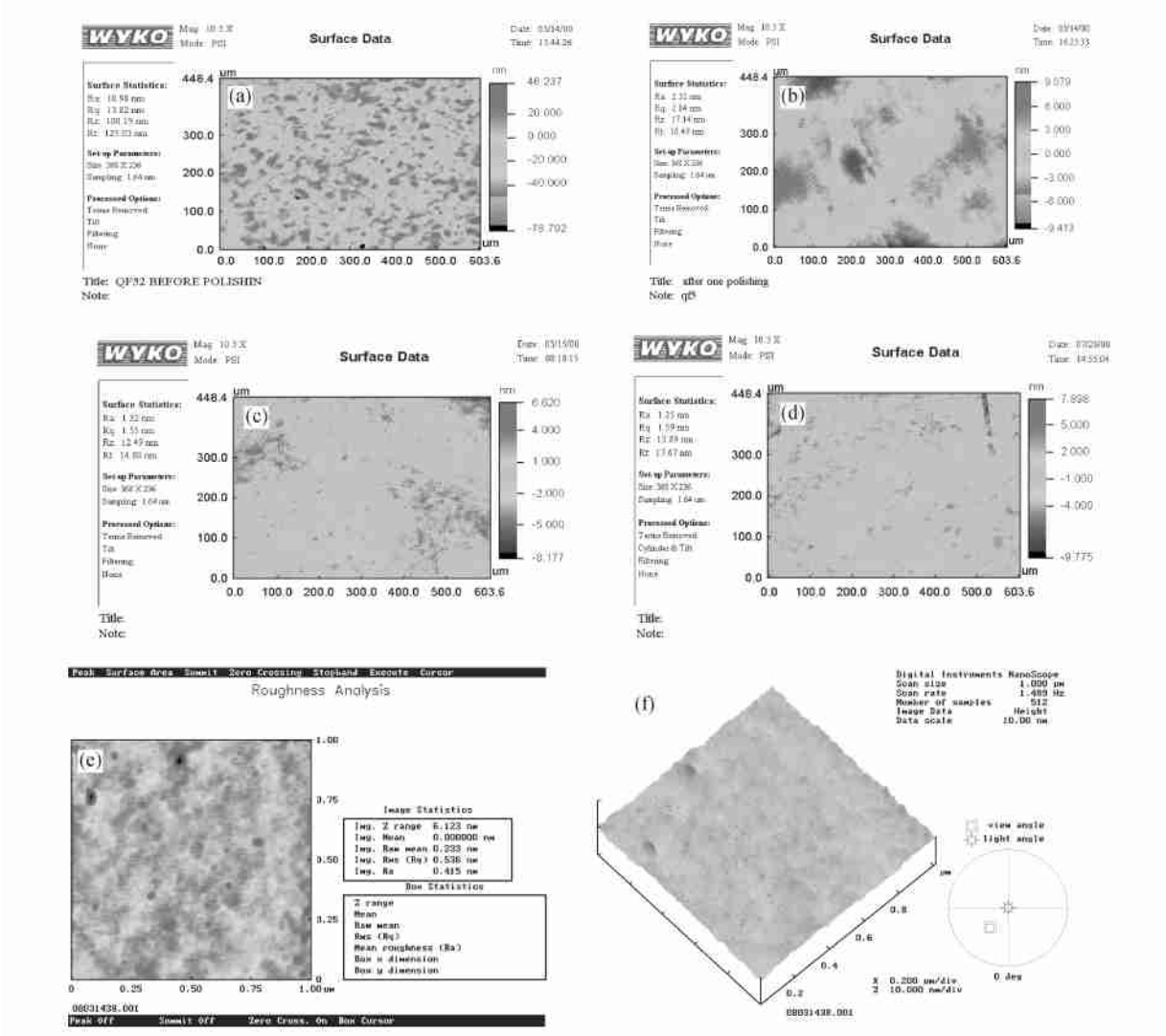

Fig. 7. Microstructures of a K9 sample after MRF. (a) Roughness before MRF (Ra=10.98 nm); (b) roughness after 10 min polishing (Ra=2.31 nm); (c) roughness after 20 min polishing (Ra=1.22 nm); (d) roughness after erosion by HF (Ra=1.25 nm); (e) short wavelength roughness after MRF (Ra=0.536 nm); (f) 3D view of short wavelength roughness.

To analyze the subsurface damage of the experimental sample after MRF, a formidable experimental condition is used: after 20 min polishing, the sample shown in Fig. 7(c) is immersed in hydrofluoric acid with 2% concentration for 2 h. The result in Fig. 7(d) shows that there is not much difference in roughness before and after immersions (from Ra=1.22 nm to Ra=1.25 nm). This indicates that a virtually damage free surface can be achieved by means of MRF.

The residual short wavelength error in the surface of the experimental sample after MRF is also an important evaluating index, which is sensitive to the application in the field of short wavelength optics that requires super smooth accuracy. An AFM measurement is carried out on a sampling area of 1 μm × 1 μm. Fig. 7(e) and (f) show that the short wavelength surface roughness of the sample after MRF is good enough for optical use. This is a convincing example to verify the practicability of MRF technique.

4 Conclusion

A new technique, called magnetorheological finishing, in computer-controlled optical surfacing for producing a high precision and subsurface damage free surface is introduced. Based on the new concept, a novel wheel shaped polishing tool is designed in-house. The material removal function is studied theoretically in view of the influence of processing parameters such as hydrodynamic pressure and magnetic pressure. The results of process simulation indicate that the material removal function closely fits the real Gaussian distribution feature. Based on the obtained theoretical model, using different controllable parameters such as size of the gap between the workpiece and polishing wheel, rotating speed of polishing wheel, and concentration of volume fraction of non-magnetic particles and polishing time, material removal rate experiments involving a parabolic mirror are designed and carried out. Results show that the material removal rate is sensitive to these four parameters. Further experiments are carried out on the surface microstructure of the workpiece after MRF, the final surface roughness with an initial value of 10.98 nm reaches 1.22 nm RMS after 20 min of MRF, and a fast convergent speed to the nanometer level is realized. The lack of subsurface damage and AFM measurement on the polished surface is also a good indication of the practicability of the MRF technique. These results demonstrate that the new CCOS technique is a promising method for manufacturing high precision, subsurface damage free and super smooth surfaces with relatively high removal rate.

References

1 Johnson R.B. Wide field of view three-mirror telescopes having a common optical axis. Optical Engineering, 1988, 27(1): 1046—1050.

2 Cheng H.B., Feng Z.J. and Wu Y.B. Fabrication of off-axis aspherical mirrors with loose abrasive point-contact machining. Key Engineering Materials, 2004, 257—258: 153—158.

3 Fahnle O.W., Hedser V.B. and Frankena H.J. Fluid jet polishing of optical surfaces. Applied Optics, 1998, 37(28): 6771—6773.

4 Paula G. Automating lens manufacturing. Mechanical Engineering, 1997, 119(3): 88—91.

5 Takino H., Shibata N. and Itoh H. Computer numerically controlled plasma chemical vaporization machining with a pipe electrode for optical fabrication. Applied Optics, 1998, 37(22): 5198—5209.

6 Jones R.A. and Rupp W.J. Rapid optical fabrication with computer-controlled optical surfacing. Optical Engineering, 1991, 30(1): 1962—1969.

7 Doughty G. and Smith J. Microcomputer-controlled polishing machine for very smooth and deep aspherical surfaces. Applied Optics, 1987, 26(2): 2421—2426.

8 Negishi M., Ando M. and Takimoto M. Studies of super-smooth polishing on aspherical surfaces. International Journal of the Japan Society for Precision Engineering (In Japanese), 1995, 29(1): 1—4.

9 Kirk N.B. and Wood J.V. Glass polishing. British Ceramic Transactions, 1994, 93(1): 25—30.

10 Suzuki H., Hara S. and Matsunaga H. Study on aspherical surface polishing using a small rotating tool-development of polishing system. International Journal of the Japan Society for Precision Engineering (In Japanese), 1993, 27(10): 1713—1717.

11 Mori Y., Yamauchi K. and Endo K. Elastic emission machining. Precision Engineering, 1987, 9(2): 123—128.

12 Soares S.F., Baseit D.R. and Black J.P. Float-polishing process and analysis of float-polished quartz. Applied Optics, 1994, 33(1): 89—95.

13 Mori Y., Yamauchi K. and Endo K. Mechanism of atomic removal in elastic emission machining. Precision Engineering, 1988, 10(1): 24—28.

14 Golini D. Magnetorheological finishing automates precision optics fabrication. Laser Focus World, 1998, 34(9): 187—190.

15 Pollicove H.M. Next generation optics manufacturing technologies. Proceedings of SPIE, 2000, 4231: 8—15.

16 Preston F.W. Glass technology. J. Soc., 1927, 11: 277—281.

17 Kordonski W.I. and Jacobs S.D. Magnetorheological finishing. Int. J. Mod. Phys., 1996, 10: 2837—2848.

18 Lemaire E., Menunier A. and Bossis G. Influence of the particle size on the rheology of magnetorheological fluids. J. Rheol., 1995, 39(5): 1011—1013.

19 Chi C.Q., Wang Z.S. and Zhao P.Z. Iron Magneto-Fluid-Mechanics, (in Chinese). Beijing: Beihang University Press, 1993: 110—119.

20 Yang P.R. Numeric Analysis of Fluid Lubrication, (in Chinese). Beijng: National Defence Industry Press, 1998: 29—36.

21 Jones R.A. Optimization of computer controlled polishing. Applied Optics, 1977, 16(1): 218—224.